(where it may mediate cell selection), GCK may, at least in part, transduce the TNF-α signal to the SAPKs.

The data in Figs 1–3 as well as direct assays[3] indicate that overexpressed GCK is constitutively active. Thus endogenous GCK may be regulated *in situ* by oligomerization, or by limiting concentrations of an inhibitor, the effects of which are relieved by upstream stimuli—processes possibly mediated by the non-catalytic GCK carboxy terminus. Thus overexpression of the GCK carboxy terminus might activate the SAPKs either by promoting GCK oligomerization or competing away an inhibitor. To begin to test this hypothesis, we generated pEBG-GCΔNT, a construct consisting of the GCK carboxy terminus fused to GST (Fig. 4*c*). Coexpression of pEBG-GCΔNT and SAPK resulted in a fivefold activation of SAPK. Anisomycin treatment of GCΔNT/SAPK coexpressing cells resulted in a further fivefold stimulation of SAPK activity (Fig. 4*d*). Expression of GCΔNT had no effect on the levels of coexpressed HA-SAPK (Fig. 4*e*). Activation of the SAPKs by the GCΔNT construct was nearly half that incurred by wild-type GCK. Thus the GCK carboxy terminus may regulate GCK activation by oligomerization or through interaction with an inhibitor.

While it is likely that multiple mechanisms of SAPK activation exist, our results show that, as in yeast[1,2,4,17,18], a mammalian member of the *STE20* family of protein kinases, GCK, can specifically regulate the SAPK pathway, an ERK-based signalling cascade. These results imply an astonishing degree of evolutionary conservation in signal transduction pathways. The activation of the SAPKs by GCK is specific inasmuch as GCK fails to activate other mammalian ERK pathways, and not all mammalian Ste20s activate the SAPKs. Our results also indicate that, like the SAPKs, GCK is activated *in situ* by TNF-α, a potent SAPK agonist[5], and that GCK activation may involve oligomerization or dissociation of an inhibitor. Activated GCK may in turn recruit the SAPKs in response to TNF-α. Although yeast genetics place the *STE20*s upstream of the MEKKs, the actual substrates of GCK are unknown. Our preliminary data indicate that GCK does not phosphorylate SEK1 directly. Moreover, we do not detect activation by GCK and MEKK1, an immediate upstream activator of SEK1 (ref. 16). The prominent expression of GCK in the follicular germinal centre suggests that the GCK/SAPK pathway may be important in the B-cell differentiation and selection that occur in the germinal centre. □

Received 18 April; accepted 7 September 1995.

1. Levin, D. E. & Errede, B. *Curr. Opin. Cell Biol.* **7,** 197–202 (1995).
2. Herskowitz, I. *Cell* **80,** 187–197 (1995).
3. Katz, P., Whalen, G. & Kehrl, J. H. *J. biol. Chem.* **269,** 16802–16809 (1994).
4. Leberer, E. *et al. EMBO J.* **11,** 4815–4824 (1992).
5. Kyriakis, J. M. *et al. Nature* **369,** 156–160 (1994).
6. Dérijard, B. *et al. Cell* **76,** 1025–1037 (1994).
7. Sánchez, I. *et al. Nature* **372,** 794–798 (1994).
8. Han, J., Lee, J.-D., Bibbs, L. & Ulevitch, R. J. *Science* **265,** 808–811 (1994).
9. Avruch, J., Zhang, X.-f. & Kyriakis, J. M. *Trends biochem. Sci.* **19,** 279–283 (1994).
10. Cowley, S., Paterson, H., Kemp, P. & Marshall, C. J. *Cell* **77,** 841–852 (1994).
11. Mansour, S. J. *et al. Science* **265,** 966–970 (1994).
12. Rouse, J. *et al. Cell* **78,** 1027–1037 (1994).
13. Freshney, N. W. *et al. Cell* **78,** 1039–1049 (1994).
14. Choi, K.-Y., Scatterberg, B., Lyons, D. M. & Elion, E. A. *Cell* **78,** 499–512 (1994).
15. Dérijard, B. *et al. Science* **267,** 682–685 (1995).
16. Yan, M. *et al. Nature* **372,** 798–800 (1994).
17. Manser, E. *et al. Nature* **367,** 40–46 (1994).
18. Martin, G. A., Bollag, G., McCormick, F. & Abo, A. *EMBO J.* **14,** 1970–1978 (1995).
19. Freisen, H., Lunz, R., Doyle, S. & Segall, J. *Genes Dev.* **8,** 2162–2175 (1994).
20. Coso, O. A. *et al. Cell* **81,** 1137–1146 (1995).
21. Minden, A. *et al. Cell* **81,** 1147–1157 (1995).
22. Bruder, J. T., Heidecker, G. & Rapp, U. R. *Genes Dev.* **6,** 545–556 (1992).
23. Lee, J. C. *et al. Nature* **372,** 739–746 (1994).

ACKNOWLEDGEMENTS. C.M.P. and J.H.K. contributed equally to this work. We thank A. S. Zervos for pMT3-p38, U. R. Rapp for pRSV-BXB-Raf-1, K. Andrabi for preliminary experiments, G. Whalen for assistance and K. Dellovo for photography. J.M.K. is supported by grants from the USPHS and the US Army Breast Cancer Research Program. T.F. is supported by the USPHS and by a Grant-in-Aid from the American Heart Association. I.S. is supported by a USPHS Training Grant awarded to the M.G.H., J.H.K. and P.K. are supported by the Arthritis Foundation and an Interagency Personnel Agreement from the NIAID.

Initial hydrophobic collapse in the folding of barstar

Vishwas R. Agashe, M. C. R. Shastry & Jayant B. Udgaonkar*

National Centre for Biological Sciences, TIFR Centre, PO Box 1234, Indian Institute of Science Campus, Bangalore 560012, India

Two models are commonly used to describe the poorly understood earliest steps of protein folding. The framework model[1–3] stresses very early formation of nascent secondary structures, which coalesce into a compact, molten, globule-like form[4,5] from which tertiary structure slowly develops[6,7]. The hydrophobic collapse model[8–10] gives overriding precedence to a nonspecific collapse of the polypeptide chain which facilitates subsequent formation of specific secondary and tertiary structure[11,12]. Here we report our analysis of the earliest observable events of the major folding pathway of barstar, a small protein. We compare the kinetics of folding using circular dichroism at 222 nm and 270 nm, intrinsic tryptophan fluorescence, fluorescence of the hydrophobic dye 8-anilino-1-naphthalene-sulphonic acid on binding, and restoration of tryptophan-dansyl fluorescence energy transfer as structure-monitoring probes. We show that the polypeptide chain rapidly collapses (within 4 ms) to a compact globule with a solvent-accessible hydrophobic core[6], but with no optically active secondary or tertiary structure. Thus the earliest event of the major folding pathway of barstar is a nonspecific hydrophobic collapse that does not involve concomitant secondary structure formation.

Rapid-mixing experiments have demonstrated that a large fraction of the final secondary structure forms in a burst phase (<10 ms)[7,13–18] of the folding pathways of all proteins studied so far. In a few cases, the secondary structure in the intermediate produced in the burst phase appears to be fluctuating and not stable[15,19,20], but it is nevertheless authentic[21]. Direct measurement of compactness of burst-phase kinetic intermediates has not yet been achieved[22], but indirect measurements indicate that they are compact[5,19,23,24] and possess sufficiently large hydrophobic clusters, formed by the collapse of non-polar residues onto each other, for binding of the hydrophobic dye 8-anilino-1-naphthalene-sulphonic acid (ANS)[6,7,16,25,26]. It has not yet been possible to ascertain, for any protein studied, whether the initial collapse of the polypeptide chain precedes or follows secondary structure formation.

The folding pathway of barstar, the inhibitor of barnase in the bacterium *Bacillus amyloliquefaciens*, has been extensively characterized[27–30]. Equilibrium-unfolded barstar comprises 69% slow-refolding (U_S) and 31% fast-refolding (U_F) molecules. The major folding pathway of barstar is $U_S \rightarrow I_{M1} \rightarrow I_{S1} \rightarrow I_N \rightarrow N$, where I_{M1}, I_{S1} and I_N are kinetic intermediates and N is the fully folded protein. In 1.0 M guanidine hydrochloride (GdnHCl), all U_S molecules fold by this pathway, and U_F molecules fold directly to N[30]. I_{M1} is a burst-phase intermediate; I_{S1} is an early intermediate with some tertiary structure because its fluorescence properties are different from those of U_S and I_{M1}; and I_N is a native-like intermediate capable, like N, of inhibiting barnase, and its transition to N probably involves *trans–cis* isomerization of the Tyr47–Pro48 peptide bond[27]. I_{M1}, I_{S1} and I_N all possess solvent-accessible hydrophobic cores on account of their ability to bind the hydrophobic dye ANS[30].

Here we have used five different spectroscopic probes to determine the chronological hierarchy of the earliest events of the major folding pathway of barstar. Folding has been performed in 1 M GdnHCl because the stabilities and therefore extents of accumulation of I_{M1}, I_{S1} and I_N are maximal at this denaturant concentration[30].

* To whom correspondence should be addressed.

TABLE 1 Kinetics of refolding of barstar in 1.0 M GdnHCl, pH 7

Spectroscopic probe	Burst-phase amplitude	λ_1 ($\times 10^3$ s^{-1})	λ_2 (s^{-1})	α_1	α_2
Ellipticity at 222 nm	0±0.12	7±3	11±4	0.3±0.1	0.7±0.1
Ellipticity at 270 nm	0±0.12	4±2	4±2	0.5±0.1	0.5 ±0.1
Intrinsic trp fluorescence	0±0.12	9±3	20±4	0.3±0.1	0.7±0.1
Fluorescence change on ANS binding	1.0				
Restoration of trp-dansyl fluorescence energy transfer	0.7±0.1	15±3	7±3	0.06±0.01	0.24±0.05

λ_1 and λ_2 are rate constants of the slow and fast kinetic phases, respectively, observed in the refolding experiments, and α_1 and α_2 are the corresponding relative amplitudes[29,30]. The burst-phase amplitude refers to the amplitude of the optical signal that occurs within the dead-time of stopped-flow mixing (<4 ms) relative to the total amplitude of the signal that is observed. When folding is monitored by a change in ANS fluorescence, the entire increase in fluorescence occurs in the burst phase, but the decrease that follows occurs in two phases with rate constants 23±4 s^{-1} and $7\times10^{-3}\pm3\times10^{-3}$ s^{-1} (Fig. 3a), corresponding in magnitude to λ_2 and λ_1, respectively[30]. Kinetic amplitudes in the single-jump experiments reported here do not reflect the relative populations of U_F and U_S, which can only be determined accurately by double-jump experiments[29]. This is because fast folding reactions occur not only in the folding pathway of U_F but also in that of U_S[27,30]. Errors shown for the kinetic parameters represent the typical deviations seen in measurements from at least three different experiments in each case.

Formation of secondary structure was monitored by measurement of the change in ellipticity at 222 nm. There is no change in ellipticity during the burst phase, within the mixing dead time (<4 ms). Thus the burst-phase intermediate I_{M1} has no optically active secondary structure. The entire change in ellipticity at 222 nm is observed upon refolding in 1.0 M GdnHCl (Fig. 1), and occurs in two kinetic phases, as described in Table 1.

Formation of tertiary structure was monitored using two different probes. The change in ellipticity in the near-ultraviolet at 270 nm is due to the gain in asymmetric environments by the aromatic residues upon refolding, and is therefore a more sensitive probe for the formation of the final tertiary structure. Figure 2*a* shows the kinetics of the change in ellipticity at 270 nm on refolding. The entire change in ellipticity at 270 nm can once again be observed, and occurs in two kinetic phases (Table 1). Figure 2*b* shows the kinetics of the increase in intrinsic trp fluorescence, as described in Table 1. As reported previously[27,29], the entire increase in trp fluorescence is observed. The increase in intrinsic trp fluorescence that occurs upon refolding is due to the increase in the quantum yield of trp fluorescence as the tryptophans are sequestered from water as the structure forms.

The hydrophobic probe ANS has been shown to bind both burst-phase intermediates and later kinetic intermediates of the folding pathways of proteins[7,16,25,26,30]. ANS binds to non-polar surfaces, presumably in the hydrophobic core, which in folding intermediates may still be solvent accessible. Such binding is therefore commonly used as a measure of the compactness of the bound intermediates[6,22]. In the case of barstar, ANS binds to the burst-phase intermediate, I_{M1}[30], which must therefore possess non-polar surfaces in a solvent-accessible hydrophobic core and is presumably compact. Figure 3*a* illustrates the kinetics of the change in ANS fluorescence during folding in 1.0 M GdnHCl. After the burst-phase increase in fluorescence on ANS binding to I_{M1}, it decreases in two phases (Table 1) as the hydrophobic core becomes inaccessible to the solvent.

To confirm that I_{M1} is indeed compact, the kinetics of the collapse of unfolded barstar molecules upon transfer to refolding conditions were determined by measurement of the kinetics of restoration of fluorescence energy transfer[23,25] between the trp residues and fluorescent dansyl labels placed on the two cys sulphydryls. Barstar has three trp residues distributed at both ends of its bundle-like structure, and thus fluorescence energy transfer averaged over all 6 trp-dansyl pairs can be used as a measure of overall compactness of the molecule[6]. On refolding, 70% of the energy transfer seen in fully folded protein is restored in a burst phase (4 ms) Fig. 3*b*. Because no increase in the intrinsic trp fluorescence quantum yield is observed in the burst phase Fig. 2*b*, this result suggests that unfolded barstar molecules collapse within 4 ms of transfer to refolding conditions. Complete energy transfer is restored in two observable kinetic phases (Table 1) which indicate either: further compaction of folding molecules; or an increase in the efficiency of energy transfer which would result from the increase in the quantum yield of trp fluorescence found to occur when the protein continues to fold after its initial collapse (Fig. 2*b* and Table 1).

Many proteins fold by means of early molten-globule intermediates, in which secondary structure appears to be stabilized in part by productive hydrophobic contacts[4,5,15,26]. In the case of

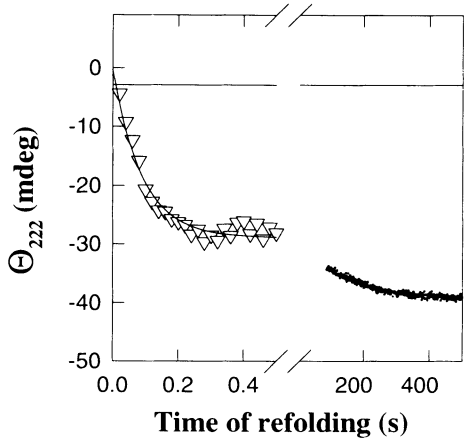

FIG. 1 Formation of secondary structure. The change in ellipticity at 222 nm with time of refolding is shown. Barstar that had been unfolded to equilibrium in 6.0 M GdnHCl was refolded in 1.0 M GdnHCl at pH 7. Two kinetic phases are seen, and the results of a nonlinear least-squares fit of the data to the sum of two exponentials are shown in Table 1. The change in ellipticity upon refolding extrapolates back to the ellipticity of the protein in 6.0 M GdnHCl at time zero, within the experimental error in the determination of the unfolded protein baseline, represented by a horizontal solid line.

METHODS. The purification of barstar has been described previously[28]. Stopped-flow circular dichroism studies of folding were performed using a Biologic SFM-3 stopped-flow machine interfaced to a Jasco J720 spectropolarimeter, using the optical and mechanical interface provided for the purpose by Jasco. A 1.5-mm pathlength FC15 cuvette was used for all circular dichroism studies. Barstar (20 μl) in unfolding buffer (6.0 M GdnHCl, 5 mM sodium phosphate, 250 μM EDTA and 300 μM DTT, pH 7) was mixed with 220 μl refolding buffer (0.55 M GdnHCl, 5 mM sodium phosphate, 250 μM EDTA and 300 μM DTT, pH 7), using a flow rate of 5 ml s^{-1}. The concentration of protein during folding was 30 μM. For data acquisition by the J720 at 222 nm, the response time was set to 16 ms. The data shown represents the average of 8 separate traces. The data were fitted using the nonlinear least-squares routine in the SigmaPlot for Windows graphics software to obtain the values of λ_1 and λ_2 shown in Table 1. In this experiment, and those shown in Figs 2 and 3, the unfolded protein baseline was obtained by diluting the unfolded protein into unfolding buffer in a similar manner.

barstar, our data indicate that I_{S1} is such an intermediate. Its formation is accompanied by the fast change in intrinsic trp fluorescence[27,30], the rate of which is similar to that of the fast change in far-ultraviolet circular dichroism (Table 1). Thus I_{S1} possesses partial secondary structure as well as partial tertiary structure.

Our data show that a very early compact, structureless globule, I_{M1}, formed by a nonspecific hydrophobic collapse, precedes the molten, globule-like intermediate I_{S1} on the folding pathway. Previous studies[30] had suggested that the hydrophobic contacts in I_{M1} were nonspecific: the ANS binding ability of I_{M1} decreases linearly and not cooperatively with an increase in concentration of GdnHCl from 1 to 2 M. We have shown I_{M1} to have no optically active secondary structure. This result is surprising

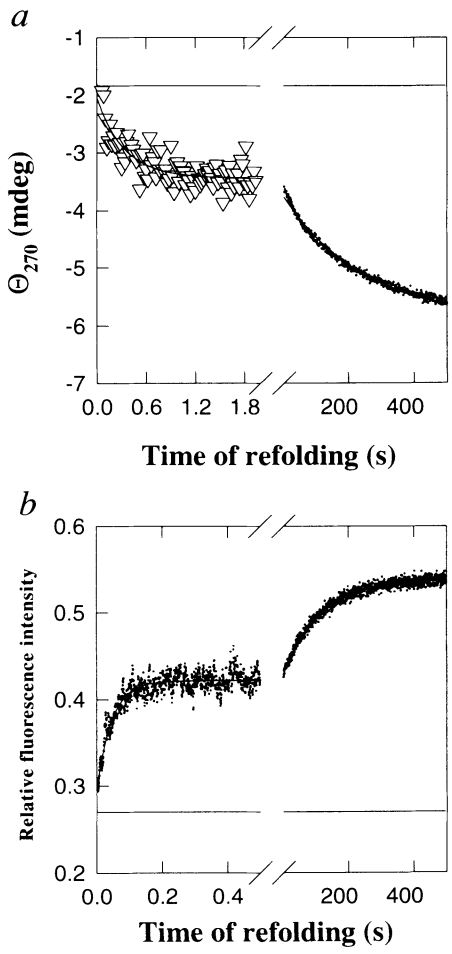

FIG. 2 Formation of tertiary structure. The changes in ellipticity at 270 nm (*a*) and fluorescence at 320 nm (*b*) with refolding are shown. Barstar that had been unfolded to equilibrium in 6.0 M GdnHCl was refolded in 1.0 M GdnHCl at pH 7. In both *a* and *b*, the horizontal solid line represents the unfolded protein baseline.
METHODS. *a*, Barstar (40 μl) in unfolding buffer (6.0 M GdnHCl, 5 mM sodium phosphate, 250 μM EDTA and 3 mM DTT, pH 7) was mixed with 200 μl refolding buffer (5 mM sodium phosphate, 250 μM EDTA, pH 7), using a flow rate of 4 ml s^{-1}. The concentration of protein during folding was 150 μM, and that of DTT was 500 μM. The data shown represent the average of 17 separately acquired traces. The values obtained for λ_1 and λ_2 by nonlinear least-squares analysis of the data are shown in Table 1. *b*, The measurement of the kinetics of folding by monitoring the change in intrinsic tryptophan fluorescence at 320 nm on excitation at 287 nm has been described previously[29,30]. The concentration of protein during refolding was 5 μM, and the buffers were the same as described for the far-ultraviolet data in Fig. 1. The values obtained for λ_1 and λ_2 by nonlinear least-squares analysis of the data are shown in Table 1.

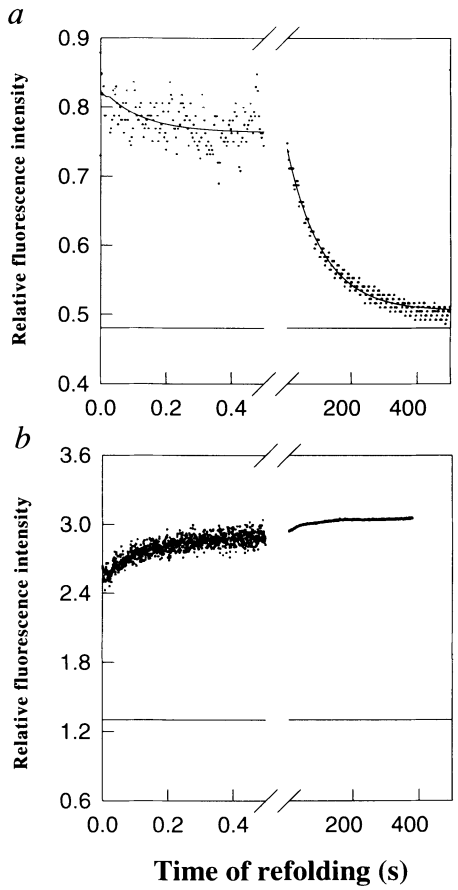

FIG. 3 Formation of a collapsed structureless globule in 1.0 M GdnHCl at pH 7. The change in ANS fluorescence at 460 nm (*a*) and restoration of trp-dansyl fluorescence energy transfer with refolding (*b*) are shown. In *a*, the ANS fluorescence for binding to fully unfolded protein in 6.0 M GdnHCl and fully folded protein in 1.0 M GdnHCl are also indicated by a horizontal solid line. In *b*, the fluorescence at 500 nm of the dansyl group bound to fully unfolded protein in 6.0 M GdnHCl is shown by a horizontal solid line to show that the efficiency of energy transfer in unfolded barstar is 40% of that in the fully folded protein.
METHODS. The use of ANS to monitor the folding kinetics of barstar has been described previously[30]. The concentration of barstar during refolding was 10 μM, and that of ANS 50 μM. The folding kinetics of barstar, when monitored by the change in intrinsic tryptophan fluorescence, are identical in the presence and absence of ANS[30]. This indicates that ANS does not perturb the folding pathway of barstar. For the fluorescence energy transfer experiments, 64 μM barstar was reacted with 3 mM 1,5 IAEDANS (5-((((2-iodoacetyl)-N-methyl)amino)ethyl)amino)naphthalene-1-sulphonic acid) in 6.0 M GdnHCl, 20 mM sodium phosphate buffer at pH 7 for 1 h. Excess dye was then removed by gel filtration using a PD-10 column (Pharmacia). The extent of labelling was determined by measurement of the absorbance of the dye bound at 337 nm, and the absorbance of the protein at 280 nm (ref. 23): for the data shown in *b*, the extent of labelling was 1 dansyl per barstar molecule. Trp fluorescence was excited at 287 nm, and dansyl fluorescence was monitored using a 500 nm Oriel bandpass filter of bandwidth 50 nm. Labelled barstar (20 μl) in unfolding buffer (6.0 M GdnHCl, 5 mM sodium phosphate, 250 μM EDTA and 100 μM DTT, pH 7) was mixed with 220 μl refolding buffer (0.55 M GdnHCl, 5 mM sodium phosphate, 250 μM EDTA, 100 μM DTT, pH 7), using a flow rate of 4 ml s^{-1}. In a control experiment, the rates of folding of the labelled protein were shown to be similar to those of unlabelled protein, when monitored by intrinsic trp fluorescence (data not shown). Another control experiment showed that the activity of the labelled protein is 75% of that of unlabelled barstar (S. Ramachandran, personal communication). In a third control experiment (data not shown), results similar to those shown here were obtained both for the relative amplitude of the burst phase and the subsequent kinetics when the extent of labelling was increased to 1.6 dansyls per barstar molecule by changing the conditions for labelling.

because, for other proteins, burst-phase intermediates display secondary structure even when folding is performed at relatively higher concentrations of denaturant than those used here[16,31]. It is unusual to find hydrophobic collapse preceding secondary structure formation for the folding of any protein in any folding condition. □

Received 31 May; accepted 4 September 1995

1. Ptitsyn, O. B. *Dokl. Akad. Nauk. SSSR* **210,** 1213–1215 (1973).
2. Kim, P. S. & Baldwin, R. L. *A. Rev. Biochem.* **51,** 459–489 (1982).
3. Udgaonkar, J. B. & Baldwin, R. L. *Nature* **335,** 694–699 (1988).
4. Ptitsyn, O. B., Pain, R. H., Semisotnov, G. V., Zerovnik, E. & Razgulyaev, D. I. *FEBS Lett.* **262,** 20–24 (1990).
5. Jennings, P. & Wright, P. E. *Science* **262,** 892–896 (1993).
6. Ptitsyn, O. B. in *Protein Folding* (ed. Creighton, T. E.) 243–300 (Freeman, New York, 1992).
7. Ptitsyn, O. B. *Protein Engng* **7,** 593–596 (1994).
8. Robson, B. & Pain, R. H. *J. molec. Biol.* **58,** 237–259 (1971).
9. Dill, K. A. *Biochemistry* **24,** 1501–1519 (1985).
10. Gutin, A. M., Abkevich, V. I. & Shakhnovich, E. I. *Biochemistry* **34,** 3066–3076 (1995).
11. Finkelstein, A. V. & Ptitsyn, O. B. *Prog. Biophys. molec. Biol.* **50,** 171–190 (1987).
12. Chan, H. S. & Dill, K. A. *J. chem. Phys.* **90,** 492–509 (1989).
13. Kuwajima, K., Yamaya, H., Miwa, S., Sugai, S. & Nagamura, T. *FEBS Lett.* **221,** 115–118 (1987).
14. Kuwajima, K., Semisotnov, G. V., Finkelstein, A. V., Sugai, S. & Ptitsyn, O. B. *FEBS Lett.* **334,** 265–268 (1993).
15. Radford, S. E., Dobson, C. M. & Evans, P. A. *Nature* **358,** 302–307 (1992).
16. Mann, C. J. & Matthews, C. R. *Biochemistry* **32,** 5282–5290 (1993).
17. Matthews, C. R. *A. Rev. Biochem.* **62,** 653–683 (1993).
18. Roder, H. & Elove, G. A. in *Mechanisms of Protein Folding* (ed. Pain, R. H.) 26–54 (IRL, New York, 1994).
19. Khorasanizadeh, S., Peters, I. D., Butt, T. R. & Roder, H. *Biochemistry* **32,** 7054–7063 (1993).
20. Varley, P. *et al. Science* **260,** 1110–1113 (1993).
21. Guijarro, J. I. *et al. Biochemistry* **34,** 2998–3008 (1995).
22. Feng, H.-P. & Widom, J. *Biochemistry* **33,** 13382–13390 (1994).
23. Kawata, Y. & Hamaguchi, K. *Biochemistry* **30,** 4367–4371 (1991).
24. Elöve, G. A., Chaffotte, A. F., Roder, H. & Goldberg, M. E. *Biochemistry* **31,** 6876–6883 (1992).
25. Semisotnov, G. V. *et al. Biopolymers* **31,** 119–128 (1991).
26. Itzhaki, L. S., Evans, P. A., Dobson, C. M. & Radford, S. E. *Biochemistry* **33,** 5212–5220 (1994).
27. Schreiber, G. & Fersht, A. R. *Biochemistry* **32,** 11195–11203 (1993).
28. Khurana, R. & Udgaonkar, J. B. *Biochemistry* **33,** 106–115 (1994).
29. Shastry, M. C. R., Agashe, V. R. & Udgaonkar, J. B. *Protein Sci.* **3,** 1409–1417 (1994).
30. Shastry, M. C. R. & Udgaonkar, J. B. *J. molec. Biol.* **247,** 1013–1027 (1995).
31. Sugawara, T., Kuwajima, K. & Sugai, S. *Biochemistry* **30,** 2698–2706 (1991).

ACKNOWLEDGEMENTS. We thank M. K. Mathew for discussion and S. Ramachandran for checking the activity of labelled protein. This work was funded by the Tata Institute of Fundamental Research and by the Department of Biotechnology, Government of India.

CORRECTION

Regulation of neural induction by the Chd and Bmp-4 antagonistic patterning signals in *Xenopus*

Yoshiki Sasai, Bin Lu, Herbert Steinbeisser & Eddy M. De Robertis

Nature **376,** 333–336 (1995)

THE PCR primer sequences for NF-M and NCAM in the legend of Fig. 1 were accidentally deleted. The primer sequences for NF-M are: F,5′-GAACAGTACGCCAAGCTGACTG, and R,5′-GCAGCAATTTCTATATCCAGAG (28 cycles); those for NCAM (accession no. M25696) are: F,5′-GCGGGTA-CCTTCTAATAGTCAC, and R,5′-GGCTTGGCTGTGGTT-CTGAAGG (28 cycles). We thank R. Harland for pointing out our mistake. □